

Supplementary Information

Lifetime Measurements of 5% Tm³⁺ doped PAA-UCNPs on Ag-HCNA and glass

The lifetimes of 5% Tm³⁺ doped PAA-DCNPs doped PAA-UCNPs, placed on glass and Ag-HCNAs to form a multilayer, were characterized using a frequency domain lifetime measurement technique with modulated pump and detection methodology, previously established in our prior work^[1-2]. In this process, the samples were excited at 1208 nm, and the emitted UCL photons at 808 nm were collected. Both the pump light and resulting UCL signals were directed through mechanical choppers to generate a near-square-wave response. To evaluate of the excited state lifetime of Tm³⁺ under square wave excitation at a frequency denoted as ' ν ' over a single modulation period ' T ' ($T = \nu^{-1}$), a 'three-level' model was employed. Assuming rapid transition of electrons from the excited ³H₄ (Tm³⁺) state to the ³H₆ (Tm³⁺) luminescent state, and maintaining a low pump rate to prevent state saturation, a single differential equation was employed to depict the population of the ³H₄ (Tm³⁺) state:

$$\frac{dN}{dt} = -\frac{N}{\tau} + R(t)N_T \quad (1)$$

Where $R(t)$ denotes the pump rate, while $R = r$ for $0 < t < T/2$ and $R = 0$ for $T/2 < t < T$. The emitted signal under continuous excitation is $S_0 = N/\tau = rN_T$. The resulting signal, $S(t) = N(t)/\tau$ is,

$$S(t) = S_0 \left(1 - \frac{e^{-t/\tau}}{1 + e^{-T/2\tau}}\right), \quad 0 < t < \frac{T}{2} \quad (2)$$

$$S(t) = S_0 \frac{e^{-(t-T/2)/\tau}}{1 + e^{-T/2\tau}}, \quad \frac{T}{2} < t < T \quad (3)$$

For a modulation frequency, ν , and integration time, t_{int} , the spectrometer integrates over νt_{int} periods. Assuming an experimental collection and detection efficiency denoted by η , when the two choppers are out of phase ($\phi = \pi$), the spectrometer measures a signal,

$$P_\pi(\nu) = \eta \nu t_{int} S_0 \int_{T/2}^T S(t) dt = \nu P_* \tanh(4\nu\tau)^{-1} \quad (4)$$

To normalize this signal, we measure the sample fluorescence without the two choppers over the same integration time, to find $P_* = \eta t_{int} S_0$. The ratio of the two measurements, $F(\nu)$, yields the lifetime,

$$F(\nu) = \frac{P_\pi(\nu)}{P_*} = \nu\tau \tanh((4\nu\tau)^{-1}) \quad (5)$$

When a collection of emitters with a mono exponential decay, the lifetime is returned for each measurement of $F(\nu)$. In the case involving mixtures of emitters with various lifetimes, the result will be an average signal,

$$P_{\pi}(\nu) = P_* \sum_i^N a_i \nu \tau_i \tanh((4\nu\tau_i)^{-1}) \quad (6)$$

Where a_i denotes the proportions of emitted photons from the emitters with lifetimes, τ_i , and $\sum_i a_i = 1$. When working with a bi-exponential decay model that accounts for the behaviour of plasmonically coupled and uncoupled DCNPs, the fitting process entails a two-emitter lifetime system. The fluorescence lifetime data was fitted using the Python package `scipy.optimize.curve_fit` version 1.11.3, developed by Scipy³. This package utilizes a non-linear least squares method to effectively fit a function to the experimental data. The selection of the fitting function was guided by the underlying physics model being investigated, and the quality of the fit is assessed through the calculation of the fitting error, as represented by the equation:

$$\chi^2 = \sum_{i=1}^n \left(\frac{y_i - f(x_i)}{\sigma_{y_i}} \right)^2 \quad (7)$$

where y_i is the value of the raw data, σ_{y_i} is the uncertainty of y_i , and $f(x_i)$ is the fitting result of each y_i .

Empirical equations from previous studies^[1-2] have demonstrated that in the unsaturated excitation region, the radiative decay rate enhancement ($\Gamma_{rad}'/\Gamma_{rad}$) and the ratio of plasmonic-modified quantum yield to the intrinsic quantum yield of UCNPs (η'/η) can be estimated using the following equations

$$I_{Ag} = N_{Tm} \times f \times \Gamma_{rad} \times E_0^{2n} + N_{Tm} \times (1-f) \times \Gamma_{rad}' \times E^{2n} \quad (8)$$

$$I_{Glass} = N_{Tm} \times \Gamma_{rad} \times E_0^{2n} \quad (9)$$

$$Enh_{total} = \frac{I_{Ag}}{I_{Glass}} = f + (1-f) \times \frac{\Gamma_{rad}'}{\Gamma_{rad}} \times \frac{E^{2n}}{E_0^{2n}} \quad (10)$$

$$\Gamma_{rad} = \eta \times \Gamma_{total} \quad (11)$$

$$\frac{\Gamma_{total}'}{\Gamma_{total}} = \frac{\Gamma_{rad}'/\eta'}{\Gamma_{rad}/\eta} = \frac{\Gamma_{rad}' \times \eta}{\Gamma_{rad} \times \eta'} \quad (12)$$

$$Enh_{total} = \frac{\Gamma_{rad}'}{\Gamma_{rad}} \times \left(\frac{E}{E_0} \right)^4 \quad (13)$$

Where I_{Glass} and I_{Ag} represent the emission intensity of Tm^{3+} induced NIR-I UCL from DCNPs on glass and on Ag-HCNA, respectively, which can be obtained from PL spectra of UCNPs on glass slide and Ag-HCNA films. N_{Tm} denotes the total number of Tm^{3+} ions distributed across the Ag-HCNA film. f signifies the fraction of Tm^{3+} minimally coupled with Ag-HCNA. Γ_{rad} and Γ'_{rad} correspond to the intrinsic and plasmonic-modified radiative decay rate of Tm^{3+} induced NIR-I UCL, respectively. E^{2n} and E_0^{2n} represent the excitation intensities of UCNPs at the hot spots and in free space, respectively, with E^{2n}/E_0^{2n} indicating the local E-field intensity enhancement. η and η' stand for the intrinsic and the plasmonic-modified quantum yield of Tm^{3+} induced NIR-I UCL. Enh_{total} represents the observed UCL enhancement factor at 808 nm. Γ_{total} and Γ'_{total} symbolize the total decay rates of both the intrinsic Tm^{3+} and plasmonic-coupled Tm^{3+} , each corresponding to the inverse of their respective lifetimes.

In this study, lifetime measurements indicated the presence of only one radiative decay channel when UCNPs were coated onto two types of Ag-HCNA films. Thus, we assumed that the observed enhanced UCL signals (Figure 3a, orange and red spectra) originated from UCNPs within the regions of enhanced local E-field, while the UCL signals from uncoupled UCNPs were negligible. Under these conditions, $f = 0$ and $n = 2$. Consequently, Equation 3 can be simplified and transformed into Equation 6.

Electromagnetic modelling and Purcell factor simulation

Electromagnetic modeling of two types of Ag hole-cap nanoarrays (Ag-HCNA) was conducted using the commercial FDTD software Lumerical. The structural parameters for Ag-HCNA(S) and Ag-HCNA(L) were based on those provided in Figure S2 and Table S1. In this FDTD model, the silver was characterized using a Drude–Lorentz model, while the PS beads and glass substrate had refractive indices of 1.54 and 1.52, respectively^[3]. Perfectly matched layers (PMLs) were applied at the upper and lower boundaries of the computational domain to minimize non-physical reflections, and periodic boundaries were implemented in the other two dimensions to simulate an infinite hexagonal array of PS nanospheres with nano-cap arrays. The FDTD cell resolution was set to 4 nm in each direction, as determined by convergence testing. Reflections, absorption, and transmission of the nanoarrays were calculated using a method previously described^{[1], [4]}, where the incident, transmitted, and backscattered fields were determined through computational surfaces placed in the glass and above the nanoarray. The nanoarray was excited using an incident plane wave normal to the upper surface with an excitation wavelength of 1208 nm.

Purcell factor simulations were also conducted using Lumerical. Three-dimensional simulations employed PML boundaries at the upper and lower boundaries, with periodic boundaries in the other two dimensions. The emitter was modeled as an electric dipole, and an overwrite mesh region with a uniform mesh size of 4 nm was used to balance simulation time and accuracy. This mesh region fully enclosed the dipole and the silver structures. Simulations of three dipoles with different orientations (aligned to the x, y, and z axes) were performed at each point, and the averaged Purcell factor was calculated by averaging the Purcell factors for these three orientations. For simplification, all points were confined to the xOz plane. The simulated configuration, as illustrated in Figure 5d,

featured dipoles positioned at four selected locations (A to D), each with a consistent perpendicular distance of 30 nm from the dipole to the Ag-HCNA surface. Specifically, Points A and D were aligned with the x and z axes, respectively, with Point A situated on the $z = 50$ nm plane and Point D on the $x = 0$ nm plane.

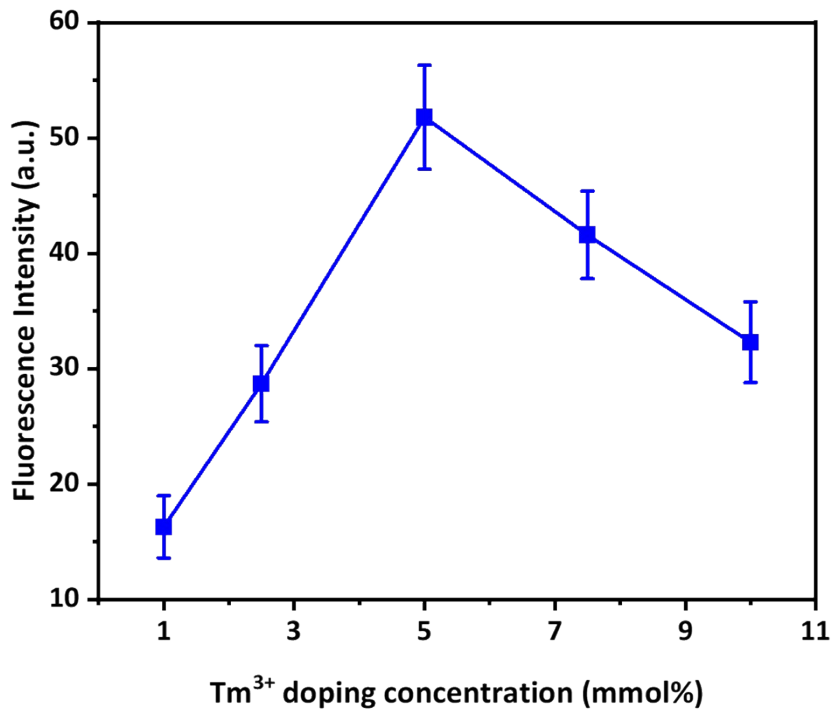


Figure S1 shows the UCL intensity of cyclohexane-dispersed Tm³⁺-doped NaYF₄ UCNP with varying Tm³⁺ doping concentrations. The 5% concentration was optimized to achieve the highest UCL performance.

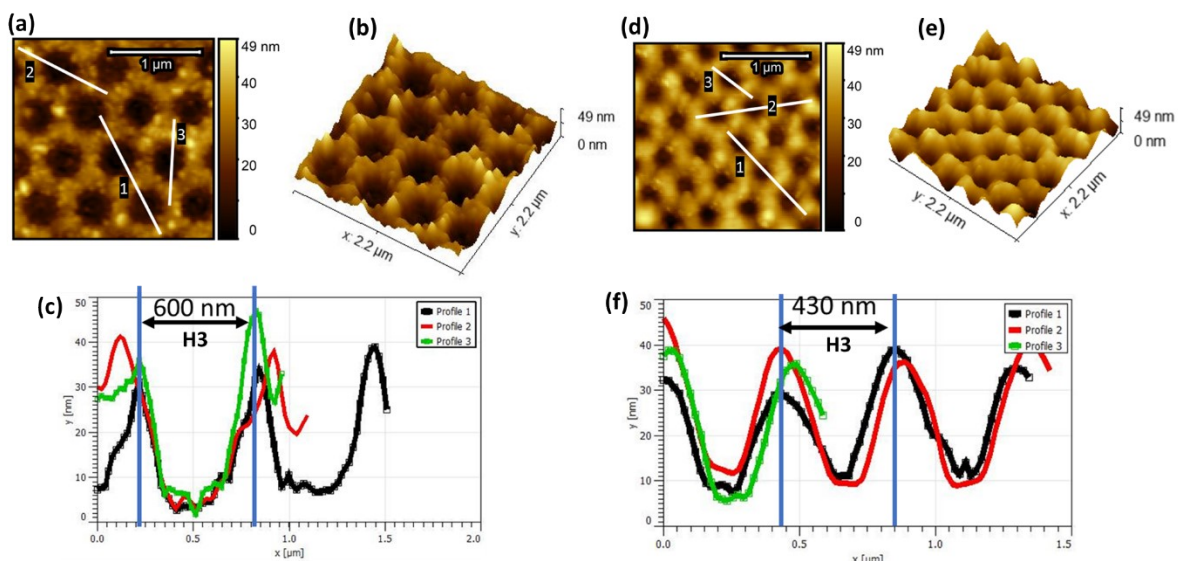


Figure S2 shows the morphological characterization of the remaining Ag nanohole film after the removal of PS beads and Ag hemisphere caps from Ag-HCNA. The figure includes AFM tapping-mode images, corresponding topographical representations, and line depth profiles

of Ag nanoholes from (a, b, c) Ag-HCNA(L) and (d, e, f) Ag-HCNA(S). (c) and (f) reveal an average Ag layer thickness of ~ 40 nm for both types of substrates. H3 denotes the diameter of the holes, measured between the apexes of adjacent holes.

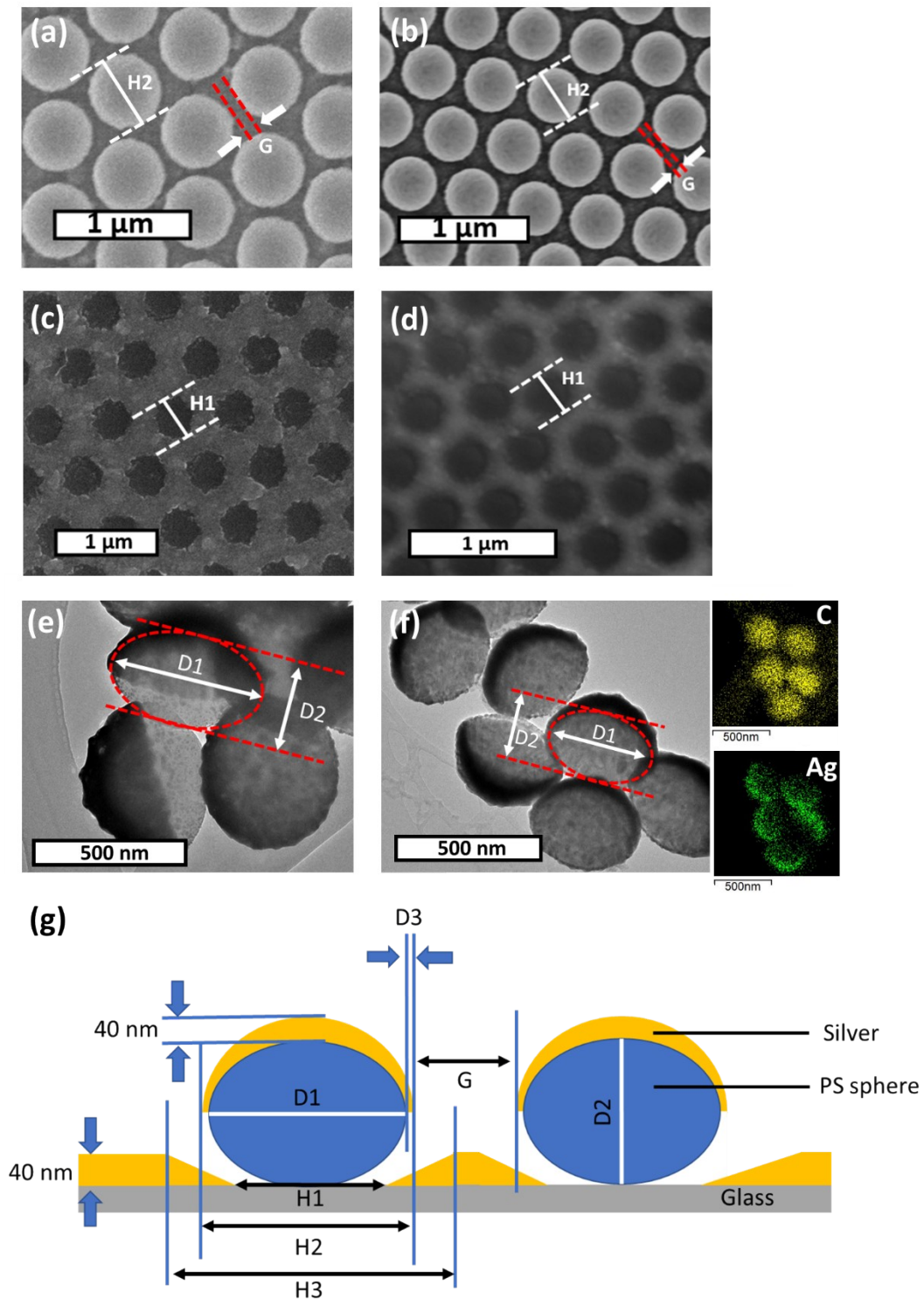


Figure S3 shows the morphological characteristics and structural parameter measurements of Ag-HCNA. (a) and (c) show SEM images and corresponding Ag nanoholes from Ag-HCNA(L), while (b) and (d) present the counterparts from Ag-HCNA(S). (e) and (f) show TEM images of individual Ag hemispherical caps and the underneath PS bead support, originated from Ag-HCNA(L) and Ag-HCNA(S), respectively, along with corresponding EDX mapping on the right of panel (f). (g) provides a schematic configuration of Ag-HCNA, featuring Ag hemisphere caps on PS spheres and the Ag nanohole base layer. D1 and D2 denote the diameters of individual PS spheres in longitudinal and transverse directions, G is the distance between adjacent Ag hemispherical caps, H1 and H3 represent the diameters measured from AFM

line depth profiles and SEM images of Ag nanoholes, and H2 denotes the diameter of the Ag hemispherical cap. D3 is equal to half the diameter difference between H2 and D1.

Table 1 Averaged structural parameters of Ag-HCNA (S) and Ag-HCNA(L), measured from Figure S2 and S3.

Sample	D1 (nm)	D2 (nm)	G (nm)	H1 (nm)	H2 (nm)	H3 (nm)
Ag-HCNA(S)	348±15	275±13	80±11	274±17	368±20	430±25
Ag-HCNA(L)	494±19	384±17	74±13	374±21	530±23	600±25

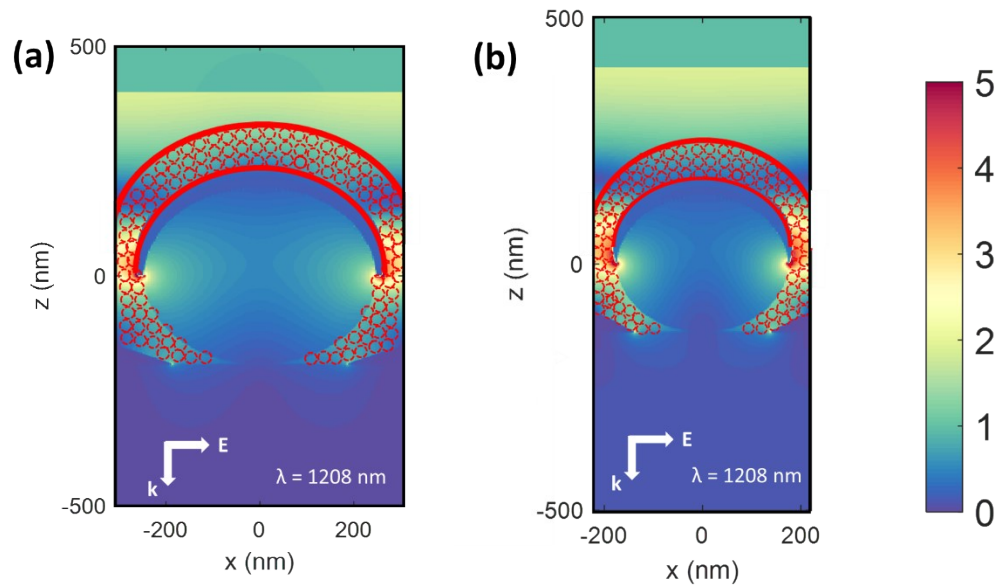


Figure S4 shows a scenario where multi-layer Tm^{3+} doped UCNP are uniformly deposited on (a) Ag-HCNA(L) and (b) Ag-HCNA(S), forming a ~ 70 nm thick layer of DCNPs, equivalent to three layers of UCNP. $\sim 15\%$ - 25% of the DCNPs are situated within a local electric field enhancement of 2-fold to 5-fold, while the remaining UCNP exhibit lower or negligible field enhancement. Red dashed circles represent UCNP with a diameter of ~ 21 nm.

Table S2 Estimated values of radiative decay enhancement (Γ'/Γ), quantum yield enhancement (η'/η) and the observed total fluorescence enhancement factor ($\text{Enh}_{\text{total}}$) for Tm^{3+} doped UCNP on Ag-HCNA(S) and Ag-HCNA(L). The local E-field amplitude (E/E_0) was assumed to be 2.5 and 3.

Sample	Tm^{3+} doped /Ag-HCNA(S)	Tm^{3+} doped /Ag-HCNA(L)
$\text{Enh}_{\text{total}}$	210	170
E/E_0	2.5	2.5
Γ'/Γ	5.4	4.4
$\Gamma'_{\text{total}}/\Gamma_{\text{total}}$	2.3	2.1
η'/η	2.3	2.1

Sample	Tm^{3+} doped /Ag-HCNA(S)	Tm^{3+} doped /Ag-HCNA(L)
$\text{Enh}_{\text{total}}$	210	170

E/E_0	3	3
Γ'/Γ	2.6	2.1
$\Gamma'_{total}/\Gamma_{total}$	2.3	2.1
η'/η	1.1	1

[1] *Advanced Optical Materials* 11.19 (2023): 2300477.

[2] *Nature Communications* 14.1 (2023): 2719.

[3] *Applied optics* 37.22 (1998): 5271-5283.

[4] Asia-Pacific Conference on Applied Electromagnetics, 2003. APACE 2003.. IEEE, 2003.